Discover Oncology

Analysis

Multidimensional investigation of thyroid hormones and prostate cancer: insights from NHANES, Mendelian randomization, genetic markers, and bioinformatics analyses

Jinhai Wu[1] · Sian Chen[1] · Ran Xu[1] · Yanfei Chen[1] · Jiadin Guo[1] · Jing Li[1] · Xiheng Zeng[1] · Bin Wang[1] · Xuejin Zhu[1]

Received: 23 January 2025 / Accepted: 12 May 2025
Published online: 21 May 2025

Abstract

Background Prostate cancer remains a major global health burden for men, with its incidence and mortality steadily rising. Thyroid hormones, critical regulators of metabolism and cell growth, have been implicated in tumorigenesis, yet their specific role in prostate cancer risk remains unclear. This study systematically investigates the relationship between thyroid hormones and prostate cancer using multidimensional approaches.

Methods A three-phase study design was employed: (1) A cross-sectional analysis of The National Health and Nutrition Examination Survey (NHANES) data to examine thyroid hormone levels (FT3 and T3) and prostate cancer risk; (2) Mendelian randomization (MR) analysis using genome-wide association studies (GWAS) data to explore causal relationships; (3) Bioinformatics analyses to annotate key Single Nucleotide Polymorphism(SNPs), identify related genes, and assess their biological roles in prostate cancer.

Results Observational analysis revealed significantly lower FT3 and T3 levels in high-risk prostate cancer patients, with adjusted models confirming an inverse association ($p < 0.001$). MR analysis supported a causal relationship between thyroid hormone replacement therapy and reduced prostate cancer risk ($b < 0$, $p < 0.05$). Four key genes—ADM5, INPP5B, NEURL4, and TYK2—were identified as downregulated in prostate cancer tissues, with prognostic and immune regulatory implications.

Conclusions Thyroid hormones exhibit a protective role against prostate cancer. ADM5, INPP5B, NEURL4, and TYK2 emerge as potential biomarkers and therapeutic targets, warranting further mechanistic and clinical validation.

Keywords Thyroid hormones · Prostate cancer · NHANES · Mendelian randomization · ADM5 · INPP5B · NEURL4 · TYK2

Abbreviations

PSA	Prostate-specific antigen
%fPSA	Percentage of free prostate-specific antigen
TSH	Thyroid-stimulating hormone
FT4	Free thyroxine

Jinhai Wu, Sian Chen and Ran Xu are contributed equally to this article.

Supplementary Information The online version contains supplementary material available at https://doi.org/10.1007/s12672-025-02672-3.

✉ Bin Wang, 972364766@qq.com; ✉ Xuejin Zhu, Xuejin_Alex@outlook.com | [1]Department of Urology, Guangzhou Institute of Cancer Research, The Affiliated Cancer Hospital, Guangzhou Medical University, Guangzhou, China.

T3	Triiodothyronine
FT3	Free triiodothyronine
PCa	Prostate cancer
NHANES	National Health and Nutrition Examination Survey
MR	Mendelian randomization
SNP	Single-nucleotide polymorphism
GWAS	Genome-wide association studies
IVs	Instrumental variables
GEPIA2	Gene expression profiling interactive analysis 2
TCGA	The cancer genome atlas
GTEx	Genotype-tissue expression
HPA	Human protein atlas
TIMER2.0	Tumor immune estimation resource 2.0
MCODE	Molecular complex detection algorithm
OR	Odds ratio
CI	Confidence interval
BMI	Body Mass Index
CRP	C-reactive protein
IVW	Inverse-variance weighted
OS	Overall survival
DFS	Disease-free survival
CAF	Cancer-associated fibroblast
AJCC	American Joint Committee on Cancer

1 Background

Prostate cancer ranks as the second most common malignancy in men worldwide [1]. Over recent years, the incidence and mortality rates of prostate cancer have been steadily rising across diverse age groups and racial populations [2]. Studies consistently demonstrate that genetic and environmental factors are critical determinants of prostate cancer development [3–6]. Established risk factors include advanced age and a family history of prostate cancer [7]. However, other modifiable risk factors contributing to prostate cancer progression remain poorly understood. Since early-stage prostate cancer is often asymptomatic, early detection and screening are pivotal for reducing mortality and improving treatment outcomes. In this context, serum prostate-specific antigen (PSA) testing has become a key tool for the early detection of potentially curable prostate cancer [8]. Elevated PSA levels are closely associated with prostate cancer progression [9] and measuring the percentage of free PSA (%fPSA) improves screening specificity [10].

Thyroid hormones play a crucial role in regulating energy balance, metabolism, and growth. Recent studies have increasingly revealed their potential impact on cancer development [11]. Evidence suggests that lower thyroid hormone levels may suppress tumor growth, whereas higher levels may promote it [12]. A prospective cohort study reported an inverse association between serum thyroid-stimulating hormone (TSH) levels and prostate cancer risk, while free thyroxine (FT4) levels were positively associated with risk [13]. Additionally, triiodothyronine (T3) hormonal treatment of human prostate cancer (PCa) cells reduced cell proliferation by induction of cellular senescence [14]. However, the specific relationship and mechanisms linking thyroid hormones and prostate cancer risk require further investigation.

The National Health and Nutrition Examination Survey (NHANES) provides a robust dataset, offering comprehensive information on health and nutrition issues in a nationally representative population. Leveraging NHANES data enables large-scale cross-sectional analyses to explore potential associations between thyroid hormones and prostate cancer risk.

Mendelian randomization (MR) analysis, an epidemiological approach utilizing genetic instrumental variables (IVs) to infer causal relationships between exposures and outcomes, minimizes confounding in observational studies and provides robust evidence for causality [15–17]. Functional annotation of MR-identified significant single nucleotide polymorphism (SNPs) enables exploration of their roles and associated genes. These genes were further analyzed for differential expression in prostate cancer tissues, survival outcomes, enrichment pathways, immune infiltration, and chromosomal localization, providing critical insights for subsequent mechanistic studies and potential therapeutic targets [18].

Supported by large-scale databases and advanced analytical methods, our study provides new insights into the role of thyroid hormones in the initiation and progression of prostate cancer. These findings lay the scientific foundation for the development of novel biomarkers and therapeutic strategies, offering potential opportunities for personalized diagnosis and treatment of prostate cancer.

2 Materials and methods

2.1 Overall study design

This study consists of three core components. In the first part, using data from NHANES and accounting for multiple potential confounders, we comprehensively investigated the associations between thyroid hormone levels, free prostate-specific antigen (fPSA), total prostate-specific antigen (tPSA), and prostate cancer risk. In the second part, summary statistics from genome-wide association studies (GWAS) were employed to analyze the causal relationship between thyroid hormone replacement therapy and prostate cancer. Finally, in the third part, functional annotation of key SNPs identified through MR was performed to explore the biological links between these SNPs and prostate cancer-related genes.

2.1.1 Observational study

This study utilized data from NHANES (2007–2010) to conduct a correlation analysis. NHANES is a nationwide health survey conducted by the Centers for Disease Control and Prevention (CDC) and the National Center for Health Statistics (NCHS). All data were publicly accessible via the NHANES official website, and informed consent was obtained from all participants. The extracted variables included free triiodothyronine (FT3), FT4, thyroglobulin antibody (TgAb), thyroglobulin (Tg), TSH, peroxidase antibody (TPOAb), T3, thyroxine (T4), tPSA, fPSA, urinary iodine, urinary creatinine, and body mass index (BMI). The study population consisted of men aged 40 years and older, with 2078 participants initially included. After initial screening, 688 participants with missing data—such as unrecorded race, smoking status, educational level, or prostate cancer risk assessment—were excluded. A total of 1390 participants met the inclusion criteria and were included in the final analysis (Fig. 1).

2.1.2 Assessment of serum PSA levels, age and PCa risk

Based on the National Comprehensive Cancer Network (NCCN) guidelines, prostate cancer risk is typically classified as low, intermediate, and high risk based on PSA levels, Gleason score, and clinical stage. Since the NHANES dataset does not include Gleason score and clinical staging information, we adapted the classification based on available PSA and age data. Participants were categorized into two groups based on %fPSA, tPSA, and age. The high-risk group included individuals aged ≥ 65 years with tPSA ≥ 4 or %fPSA ≤ 0.25 and tPSA ≥ 4. The low-risk group consisted of participants with %fPSA > 0.25 and tPSA < 4 [19, 20].

2.1.3 Covariate information

Baseline data of participants were collected through questionnaires and laboratory assessments, including the following variables: Smoking Status: Participants were categorized into three groups based on smoking history: never smokers (fewer than 100 cigarettes in a lifetime), former smokers (more than 100 cigarettes in a lifetime but currently not smoking), and current smokers (more than 100 cigarettes in a lifetime and currently smoking). Body Mass Index (BMI): Participants were classified as underweight (BMI < 18), normal weight ($18 \leq$ BMI ≤ 25), or overweight (BMI > 25). Race: Participants were grouped into non-Hispanic White, non-Hispanic Black, and Other Race to evaluate potential racial differences in health outcomes. Education Level: Participants were stratified into two groups: less than high school and high school or higher. This indicator is widely considered a proxy for socioeconomic status and significantly influences health behaviors and outcomes. Marital Status: Participants were classified as never married, married/living with a partner, or separated. Marital status affects both mental health and social support levels.

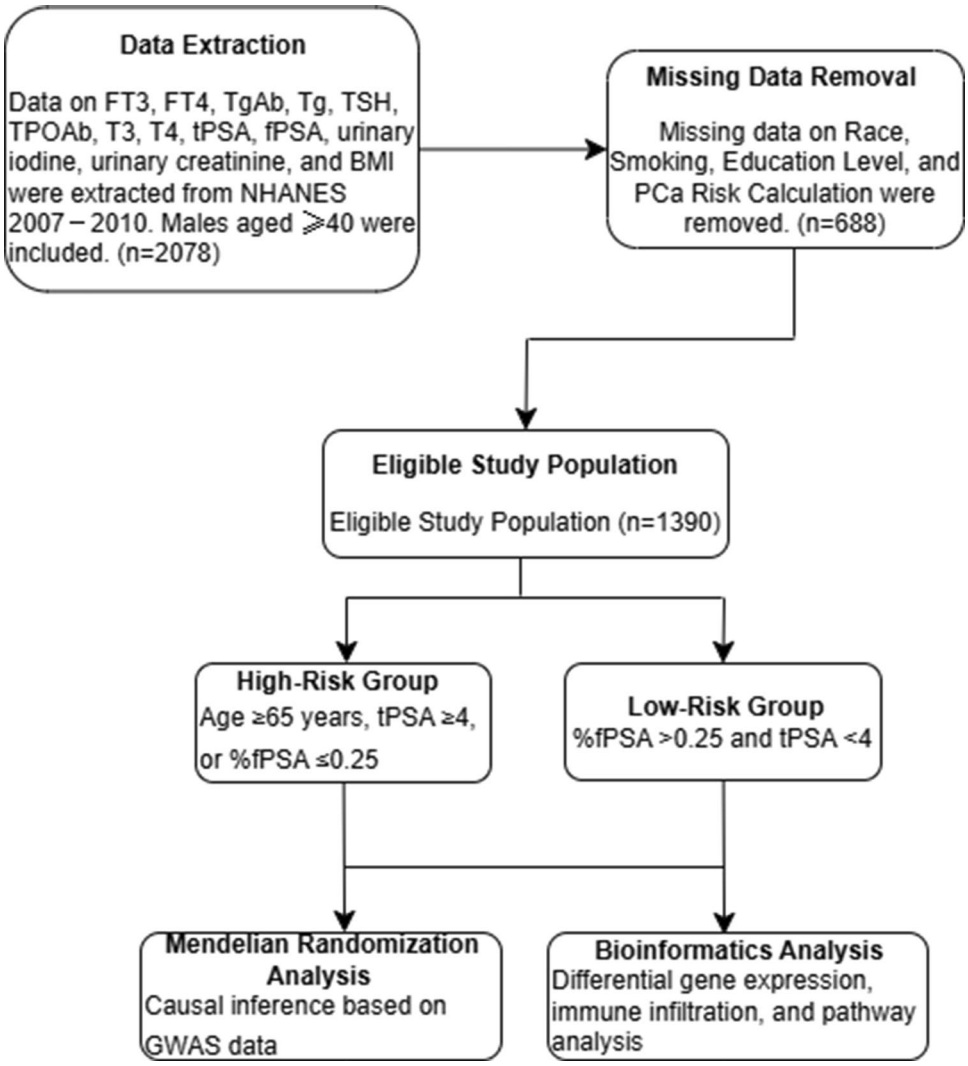

Fig. 1 Study design flowchart

2.1.4 Statistical analysis

In accordance with NHANES analytical guidelines, sample weights, strata, and primary sampling units (PSUs) were incorporated into the statistical analysis to ensure nationally representative results. Weighted t-tests were conducted for continuous variables, and weighted chi-square tests were used for categorical variables to assess differences between groups. FT3 and T3 were analyzed as continuous variables and further categorized into quartiles using equal-frequency binning. Multivariable linear regression models were applied to calculate adjusted β coefficients and 95% confidence intervals (CIs) to evaluate the associations of FT3 and T3 with serum PSA levels. Additionally, multivariable logistic regression models were used to estimate adjusted odds ratios (ORs) and 95% CIs to assess the associations of FT3 and T3 with PCa risk. Univariate and multivariable logistic regression models were employed to evaluate the ORs and 95% CIs for the relationships between thyroid-related hormones and PCa. To address potential confounding factors, a Cox proportional hazards model (COXPH) was used to evaluate the independent association between thyroid hormone levels and prostate cancer risk. Age and PSA levels were treated as continuous variables, and BMI was included as a covariate to account for its potential effect on PSA levels. Continuous variables were reported as means and ± standard deviations (SD), while categorical variables were presented as frequencies and percentages. All statistical analyses were performed using DecisionLinnc 1.0 software (Statsape Co. Ltd, Hangzhou, China) [21], and a p-value < 0.05 was considered statistically significant.

2.2 Mendelian randomization

2.2.1 Study design

This study employed univariable MR analysis to investigate the causal relationship between thyroid medication use and prostate cancer risk. To ensure that the fundamental assumptions required for MR analysis were satisfied [22], the following conditions were verified: (1) genetic variants (SNPs) are significantly associated with Medication use (thyroid preparations); (2) genetic variants are not associated with potential confounders; (3) genetic variants influence the outcome (prostate cancer) solely through their effects on Medication use (thyroid preparations).

2.2.2 Genetic instrument selection

Genetic IVs were selected from GWAS. First, genome-wide significant SNPs ($p < 5 \times 10^{-8}$) associated with medication use (thyroid preparations) were identified. Second, SNPs in linkage disequilibrium ($r^2 < 0.001$, window size < 10,000 kb) were excluded, and the remaining SNPs were retained for outcome analysis. Third, the F-statistic of each SNP was calculated to ensure strong instrument strength ($F > 10$), and weak instruments were excluded. Finally, the validity and robustness of the instrumental variables were further verified using MR Steiger filtering and the MR-PRESSO method. Detailed information on the selected genetic instrumental variables is provided in the supplementary table.

2.2.3 Outcome data

The data for both exposure and outcome variables were derived from summary statistics of GWAS. The outcome dataset included genomic data from prostate cancer cases and controls, with all participants of European ancestry. To ensure causal interpretability of the results, SNPs directly associated with the outcome variable ($p < 5 \times 10^{-5}$) were excluded from the analysis.

2.2.4 Statistical analysis

MR analysis was performed using the TwoSampleMR R package. Inverse-variance weighted (IVW) method was used as the primary analytical approach to estimate the causal effect between the exposure and the outcome. Sensitivity analyses, including the weighted median method and MR-Egger regression, were conducted to assess horizontal pleiotropy and ensure model robustness [23]. Cochran's Q test was used to evaluate heterogeneity, while the MR-Egger intercept test was performed to detect pleiotropy. Additionally, leave-one-out (LOO) analysis was carried out to identify the influence of individual SNPs on the model results. A p-value of < 0.05 was considered statistically significant.

2.3 Bioinformatics analysis

2.3.1 SNP functional annotation analysis

Functional annotation analysis of key SNPs identified in the MR analysis was performed using the Variant Effect Predictor (VEP) tool available on the Ensembl platform (www.ensembl.org). VEP is a versatile and robust tool that annotates the potential biological effects of genomic variants and provides detailed information about variant locations, associated genes, and their possible functions [24]. This process facilitated the identification of genes corresponding to the SNPs.

2.3.2 GEPIA2 analysis

GEPIA2 (http://gepia.cancer-pku.cn/index.html) is a comprehensive online analysis platform that utilizes RNA sequencing data from The Cancer Genome Atlas (TCGA) and the Genotype-Tissue Expression (GTEx) project [25]. The GEPIA2 analysis tool was used to investigate differential expression of the identified genes between prostate

cancer and normal tissues. Additionally, overall survival (OS) and disease-free survival (DFS) analyses were performed for genes with significant expression differences to identify potential target genes.

2.3.3 Metascape functional enrichment analysis

Metascape (http://metascape.org/gp/index.html#/main/step1) is a comprehensive bioinformatics tool that integrates over 40 unique biological databases to provide interactive analyses and gene annotation, among other features [26]. Metascape was used to perform rapid gene expression profiling and functional enrichment analysis of the identified differentially expressed genes.

2.3.4 Expression of related genes at the translation level

The Human Protein Atlas (HPA) (https://www.proteinatlas.org/) [27] aims to generate antibodies targeting all major isoforms of human proteins, establish a comprehensive database of protein expression patterns, and identify clinically relevant biomarkers. HPA was used to validate the protein expression levels of the target genes in normal prostate tissues and prostate cancer tissues.

2.3.5 TIMER2.0 analysis

The TIMER2.0 database (http://gepia2.cancer-pku.cn/#index) provides analytical tools for investigating immune infiltration across various tumor types [28]. This study utilized data from TCGA, including 32 tumor types and over 10,000 samples, to explore the correlation between gene expression and immune cell infiltration levels in prostate cancer. The analysis focused on the expression of biomarker genes associated with tumor-infiltrating immune cells, including B cells, CD4 + T cells, CD8 + T cells, myeloid dendritic cells, macrophages, neutrophils, monocytes, cancer-associated fibroblasts, and natural killer (NK) cells.

2.3.6 Association between gene expression and pathological staging

cBioPortal for Cancer Genomics (http://cbioportal.org) is an open-access resource that provides an integrated view of cancer genomics datasets, allowing researchers to efficiently explore mutations, copy number variations, expression differences, and associated clinical information for specific genes [29]. Using data from cBioPortal [30], we analyzed the mRNA expression levels of the target genes across different pathological stages of prostate cancer.

3 Results

3.1 General characteristics of NHANES

Baseline data for 1390 male participants were summarized (Table 1). Among them, 1212 participants were classified into the low-risk PCa group, while the remaining 178 were categorized into the high-risk PCa group. In the high-risk group, the mean level of FT3 was significantly lower at 2.977 pg/mL compared to 3.163 pg/mL in the low-risk group ($p < 0.001$). Similarly, total T3 levels showed a decreasing trend in the high-risk group (103.365 ng/dL vs. 111.095 ng/dL), with this difference also being statistically significant ($p < 0.001$). The initial analysis demonstrated a significant negative correlation between FT3 and T3 levels and prostate cancer risk. After adjusting for age, BMI, and PSA levels as continuous variables, the association between FT3 and prostate cancer risk remained positive but did not reach statistical significance (HR = 1.496, 95% CI: 0.868–2.580, $p = 0.147$) (Table 2). Similarly, T3 showed a borderline positive association with prostate cancer risk (HR = 1.008, 95% CI: 1.000–1.015, $p = 0.052$). BMI was significantly associated with an increased risk of prostate cancer (HR = 1.030, 95% CI: 1.001–1.061, $p = 0.046$). More importantly, tPSA remained a strong independent predictor of prostate cancer risk after adjusting for potential confounders (HR = 1.070, 95% CI: 1.059–1.081, $p < 0.001$).

Continuous variables are presented as mean values with standard deviations (SD). The p-values for continuous variables were calculated using weighted T-tests, whereas weighted Chi-squared tests were applied to categorical variables. The symbol 'N' represents the sample size; unweighted counts and weighted percentages are provided.

Table 1 Baseline Characteristics of Men at High Risk for Prostate Cancer Aged 40 Years and Older in the NHANES 2007–2010

Variable names	Level	Overall	PCa low risk	PCa high risk	p
n		1390	1212	178	
AGE		59.576 (12.388)	58.130 (12.137)	69.427 (9.189)	< 0.001
CRP (mg/dL)		0.367 (0.738)	0.347 (0.629)	0.501 (1.245)	0.172
FT3 (pg/mL)		3.139 (0.351)	3.163 (0.347)	2.977 (0.335)	< 0.001
FT4 (ng/dL)		0.782 (0.146)	0.780 (0.148)	0.798 (0.136)	0.070
TGN (ng/mL)		14.791 (57.199)	14.764 (60.731)	14.978 (20.991)	0.541
TSH (μIU/mL)		2.031 (1.454)	2.024 (1.453)	2.074 (1.460)	0.471
TPO (IU/mL)		13.852 (70.203)	12.760 (64.677)	21.287 (99.962)	0.515
T3 (ng/dL)		110.105 (22.298)	111.095 (22.292)	103.365 (21.196)	< 0.001
T4 (μg/dL)		7.679 (1.536)	7.656 (1.515)	7.833 (1.671)	0.285
BMI (kg/m^2)		28.920 (5.465)	28.976 (5.411)	28.539 (5.823)	0.029
Iodine, urine (μg/L)		343.662 (1322.425)	351.705 (1401.364)	288.894 (533.055)	0.577
Creatinine, urine (mg/dL)		131.763 (73.356)	131.771 (71.594)	131.708 (84.611)	0.208
tPSA (ng/mL)		1.865 (3.459)	0.957 (0.725)	8.044 (6.802)	< 0.001
%fPSA		0.349 (0.111)	0.371 (0.096)	0.200 (0.089)	< 0.001
fPSA (ng/mL)		0.477 (0.537)	0.336 (0.243)	1.434 (0.893)	< 0.001
Race (%)	Non-Hispanic White	744 (53.53)	650 (53.63)	94 (52.81)	0.216
Race (%)	Non-Hispanic Black	240 (17.27)	200 (16.50)	40 (22.47)	
Race (%)	Other Race	406 (29.21)	362 (29.87)	44 (24.72)	
Education level (%)	< High school	422 (30.36)	367 (30.28)	55 (30.90)	0.617
Education level (%)	≥ High school	968 (69.64)	845 (69.72)	123 (69.10)	
Marriage (%)	Never married	97 (6.98)	87 (7.18)	10 (5.62)	0.189
Marriage (%)	Married/Living with partner	1005 (72.30)	888 (73.27)	117 (65.73)	
Marriage (%)	Separated	288 (20.72)	237 (19.55)	51 (28.65)	
BMI (%)	Under weight	11 (0.79)	7 (0.58)	4 (2.25)	0.001
BMI (%)	Normal weight	1067 (76.76)	939 (77.48)	128 (71.91)	
BMI (%)	Overweight	312 (22.45)	266 (21.95)	46 (25.84)	
Smoke (%)	Never	566 (40.72)	490 (40.43)	76 (42.70)	0.152
Smoke (%)	Former	547 (39.35)	470 (38.78)	77 (43.26)	
Smoke (%)	Current	277 (19.93)	252 (20.79)	25 (14.04)	

Table 2 Multivariable Cox proportional hazards model for predicting prostate cancer risk

Variable Names	b	SE	HR	95%CI	p
BMI	0.03	0.015	1.03	1.001–1.061	0.046
FT3	0.403	0.278	1.496	0.868–2.580	0.147
T3	0.008	0.004	1.008	1.000–1.015	0.052
tPSA	0.068	0.005	1.07	1.059–1.081	< 0.001

3.2 Association between the FT3, T3 and serum PSA levels

Table 3 presents a linear regression analysis of the association between thyroid hormone levels (T3 and FT3) and serum prostate-specific antigen (PSA) levels. Analysis of FT3 levels showed that in the unadjusted model, there was a significant negative correlation between continuous FT3 and tPSA (b = − 1.16, 95% CI: − 1.60 to − 0.74, p-value < 0.001). This inverse relationship strengthened with higher quartiles of FT3, showing a significant negative trend (p for trend < 0.001). Model 1, adjusted for race, education, marital status, and BMI, maintained the significant inverse correlation (b = − 1.13, 95% CI: − 1.59 to − 0.67, p-value < 0.001). Model 2, further adjusted for smoking, urinary iodine, creatinine, and CRP, also sustained this negative correlation (b = − 1.05, 95% CI: − 1.45 to − 0.65,

Table 3 Associations between T3 and FT3 Levels and serum PSA in Men Aged 40 Years and Older: A Linear Regression Analysis from the NHANES 2007–2010

		Continuous FT3	Quartiles of FT3 levels				p for trend
			Q1	Q2	Q3	Q4	
tPSA	crude	− 1.16 (− 1.60, − 0.74) p-value < 0.001	Reference	− 0.57 (− 1.04, − 0.10) p-value = 0.017	− 0.80 (− 1.34, − 0.27) p-value = 0.004	− 1.03 (− 1.52, − 0.55) p-value < 0.001	< 0.001
	Model 1	− 1.13 (− 1.59, − 0.67) p-value < 0.001	Reference	− 0.50 (− 0.93, − 0.07) p-value = 0.025	− 0.73 (− 1.26, − 0.21) p-value = 0.008	− 1.00 (− 1.47, − 0.53) p-value < 0.001	< 0.001
	Model 2	− 1.05 (− 1.45, − 0.65) p-value < 0.001	Reference	− 0.56 (− 1.12, − 0.01) p-value = 0.048	− 0.79 (− 1.44, − 0.138) p-value = 0.021	− 1.09 (− 1.87, − 0.32) p-value = 0.008	< 0.001
fPSA	crude	− 0.28 (− 0.37, − 0.19) p-value < 0.001	Reference	− 0.12 (− 0.20, − 0.04) p-value = 0.003	− 0.19 (− 0.26, − 0.12) p-value < 0.001	− 0.23 (− 0.31, − 0.15) p-value < 0.001	< 0.001
	Model 1	− 0.27 (− 0.36, − 0.17) p-value < 0.001	Reference	− 0.11 (− 0.19, − 0.03) p-value = 0.007	− 0.18 (− 0.26, − 0.10) p-value < 0.001	− 0.22 (− 0.30, − 0.14) p-value < 0.001	< 0.001
	Model 2	− 0.25 (− 0.34, − 0.16) p-value < 0.001	Reference	− 0.11 (− 0.19, − 0.04) p-value = 0.006	− 0.17 (− 0.25, − 0.10) p-value < 0.001	− 0.20 (− 0.28, − 0.13) p-value < 0.001	< 0.001
		Continuous T3	Quartiles of T3 levels				p for trend
			Q1	Q2	Q3	Q4	
tPSA	crude	− 0.01 (− 0.02, − 0.002) p-value = 0.010	Reference	− 0.57 (− 0.83, − 0.31) p-value < 0.001	− 0.44 (− 0.71, − 0.16) p-value = 0.003	− 0.59 (− 1.01, − 0.16) p-value = 0.008	< 0.001
	Model 1	− 0.01 (− 0.01, − 0.001) p-value = 0.023	Reference	− 0.11 (− 0.19, − 0.04) p-value = 0.006	− 0.17 (− 0.25, − 0.10) p-value < 0.001	− 0.21 (− 0.28, − 0.13) p-value < 0.001	0.045
	Model 2	− 0.006 (− 0.01,0.001) p-value = 0.08	Reference	− 0.51 (− 0.79, − 0.24) p-value = 0.001	− 0.32 (− 0.64, − 0.01) p-value = 0.045	− 0.44 (− 0.96,0.07) p-value = 0.087	0.157
fPSA	crude	− 0.002 (− 0.003, − 0.001) p-value < 0.001	Reference	− 0.11 (− 0.18, − 0.04) p-value = 0.001	− 0.10 (− 0.17, − 0.04) p-value = 0.003	− 0.15 (− 0.23, − 0.08) p-value < 0.001	< 0.001
	Model 1	− 0.002 (− 0.003, − 0.001) p-value < 0.001	Reference	− 0.10 (− 0.17, − 0.04) p-value = 0.003	− 0.08 (− 0.16, − 0.02) p-value = 0.018	− 0.14 (− 0.22, − 0.06) p-value = 0.002	0.002
	Model 2	− 0.002 (− 0.003, − 0.001) p-value < 0.001	Reference	− 0.10 (− 0.16, − 0.04) p-value = 0.004	− 0.08 (− 0.15, − 0.01) p-value = 0.026	− 0.12 (− 0.20, − 0.04) p-value = 0.005	0.007

Crude: no covariates were adjusted

Model 1: Race, Education level, Marriage, BMI

Model 2: Race, Education level, Marriage, BMI, Smoke, Iodine urine, Creatinine urine, CRP

p-value < 0.001). For fPSA, the crude model revealed a consistent negative correlation with continuous FT3 levels (b = − 0.28, 95% CI: -0.37 to -0.19, p-value < 0.001). Similar negative correlations were maintained in Models 1 and 2.In the analysis of T3 levels, the crude model indicated a weak inverse correlation with tPSA (b = − 0.01, 95% CI: − 0.02 to − 0.002, p-value = 0.010), with this trend diminishing in Models 1 and 2 (p for trend 0.045 and 0.157, respectively). Analysis across models demonstrated a stable inverse relationship between T3 levels and fPSA, with significant trends observed in the crude, Model 1, and Model 2 (p for trend < 0.001 in all).

3.3 Association between the FT3,T3 and PCa risk

Table 4 presents the association between thyroid hormone levels (T3 and FT3) and the PCa risk using logistic regression analysis. In the unadjusted model, a significant positive association was found between continuous FT3 levels and increased PCa risk (OR = 0.19, 95% CI: 0.10 to 0.37, p-value < 0.001). Furthermore, as FT3 levels increased by quartiles, the PCa risk progressively decreased, showing a statistically significant trend (p for trend < 0.001). This trend persisted in Model 1, which adjusted for race, education, marital status, and BMI (p for trend < 0.001), and was similarly observed in Model 2, further adjusted for smoking, urinary iodine, creatinine, and CRP (p for trend < 0.001).The crude model revealed a significant inverse relationship between continuous T3 levels and PCa risk (OR = 0.98, 95% CI: 0.97 to 0.99, p-value = 0.008), with each unit increase in T3 decreasing PCa risk by 2%. Across T3 quartiles, except for the highest, risk was lower compared to the reference quartile (Q1), with an overall trend of decreasing PCa risk with

Table 4 Associations between T3 and FT3 Levels with the Risk of Prostate Cancer Among Men Aged 40 Years or Older: Logistic Regression Analysis of the NHANES 2007–2010

		Continuous FT3	Quartiles of FT3 levels				p for trend
			Q1	Q2	Q3	Q4	
PCa risk	Crude	0.19 (0.10,0.37) p-value < 0.001	Reference	0.64 (0.42,0.98) p-value = 0.04	0.32 (0.17,0.60) p-value < 0.001	0.30 (0.15,0.60) p-value = 0.001	< 0.001
	Model 1	0.21 (0.10,0.41) p-value < 0.001	Reference	0.68 (0.43,1.07) p-value = 0.095	0.33 (0.18,0.65) p-value = 0.002	0.31 (0.16,0.62) p-value = 0.002	< 0.001
	Model 2	0.21 (0.11,0.42) p-value < 0.001	Reference	0.66 (0.42,1.06) p-value = 0.083	0.35 (0.18,0.68) p-value = 0.003	0.33 (0.17,0.65) p-value = 0.003	< 0.001
		Continuous T3	Quartiles of T3 levels				p for trend
			Q1	Q2	Q3	Q4	
PCa risk	Crude	0.98 (0.97,0.99) p-value = 0.008	Reference	0.38 (0.24,0.62) p-value < 0.001	0.56 (0.34,0.92) p-value = 0.024	0.39 (0.19,0.80) p-value = 0.013	0.023
	Model 1	0.98 (0.97,0.99) p-value = 0.018	Reference	0.40 (0.25,0.64) p-value < 0.001	0.59 (0.34,1.02) p-value = 0.061	0.41 (0.19,0.88) p-value = 0.025	0.047
	Model 2	0.98 (0.97,0.99) p-value = 0.032	Reference	0.40 (0.24,0.67) p-value = 0.002	0.62 (0.35,1.09) p-value = 0.09	0.44 (0.20,0.98) p-value = 0.046	0.084

Crude: no covariates were adjusted

Model 1: Race, Education level, Marriage, BMI

Model 2: Race, Education level, Marriage, BMI, Smoke, Iodine urine, Creatinine urine, CRP

increasing T3 levels (p for trend = 0.023).This trend remained statistically significant in Model 1 and was maintained in Model 2, although the p for trend increased to 0.084. The restricted cubic spline (RCS) model, shown in Fig. 2, indicates that both T3 and FT3 are significantly associated with PCa risk, primarily exhibiting a linear relationship.

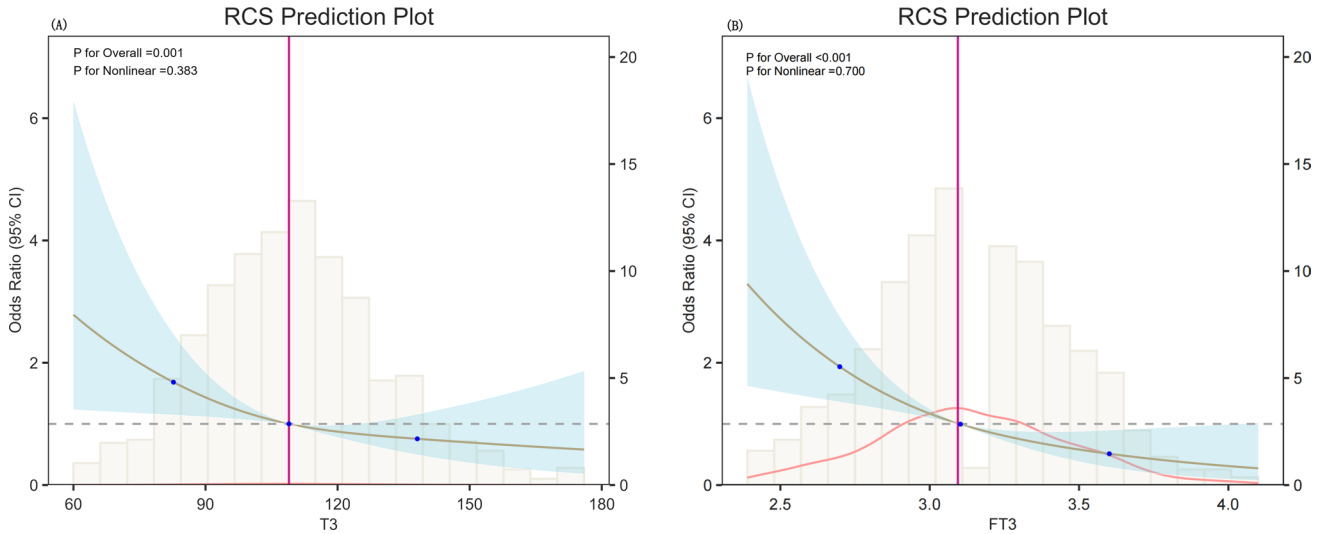

Fig. 2 Restricted spline regression curves showing the association between T3, FT3, and prostate cancer risk. **A** Illustrates the association between T3 levels and PCa risk, while **B** depicts the relationship for FT3. The horizontal axes represent the respective T3 and FT3 levels, while the vertical axes show the OR and their 95% CI, indicated by shaded areas. The reference line (OR = 1) denotes baseline risk. Histograms reflect the distributions of T3 and FT3 levels within the sample. The analysis reveals significant associations of both T3 (P for Overall = 0.001, P for Nonlinear = 0.383) and FT3 (P for Overal < 0.001, P for Nonlinear = 0.700) with prostate cancer risk, predominantly demonstrating linear relationships. Elevated risks are observed at lower T3 and FT3 levels, decreasing progressively with higher concentrations, and stabilizing thereafter

3.4 Mendelian randomization analysis

Given the limitations of cross-sectional studies in establishing causality, we employed MR analysis to explore the causal directionality. Medication use (thyroid preparations) (ebi-a-GCST90018990) was analyzed as the exposure variable, while prostate cancer outcomes (ebi-a-GCST006085, ebi-a-GCST90018905, finn-b-C3_PROSTATE, ieu-b-85) served as the outcome data. Based on predefined selection criteria, 115, 118, 116, and 113 IVs were identified for ebi-a-GCST006085, ebi-a-GCST90018905, finn-b-C3_PROSTATE, and ieu-b-85, respectively, to evaluate the potential causal relationship between thyroid medication use and prostate cancer risk (Table 5). Genetic instruments were selected based on their association with thyroid medication use, excluding those with pleiotropy or linkage disequilibrium (Dataset_1). IVW analysis demonstrated a significant inverse causal relationship between thyroid medication use and prostate cancer risk ($b < 0$, $p < 0.05$), a finding further supported by funnel plot evidence (Fig. 3).

This figure illustrates the distribution of effect estimates for single-nucleotide polymorphisms (SNPs) in the MR analysis, aimed at assessing potential biases. The funnel plot reflects the relationship between effect sizes and standard errors across different studies, where smaller standard errors correspond to effect estimates closer to the center of the plot, while larger standard errors are scattered toward the edges. Symmetrical distribution suggests the absence of significant selective bias, whereas asymmetry may indicate the presence of publication bias or other systematic errors. The subpanels represent distinct exposure-outcome pairs: (A) ebi-a-GCST90018990—ebi-a-GCST90018905; (B) ebi-a-GCST90018990—finn-b-C3_PROSTATE; (C) ebi-a-GCST90018990—ieu-b-85_00; (D) ebi-a-GCST90018990—ebi-a-GCST006085.

3.5 SNP functional annotation analysis

To further explore the potential function and biological significance of the SNPs identified in the MR analysis, we conducted a systematic functional annotation analysis. After deduplication, 462 highly relevant SNPs were filtered to yield 119 independent SNPs. Functional annotation was performed using the VEP tool provided by the Ensembl database, identifying the genomic locations, potential functional effects, and associations of each SNP with diseases or phenotypes. Consequently, 122 target genes were identified for subsequent analysis (Dataset_2).

3.6 Differential gene expression and associated survival analysis, with protein-level validation

Using GEPIA2, the expression differences of the selected 122 genes between prostate cancer and normal tissues were analyzed, resulting in the identification of 10 differentially expressed genes: ADM5, CPT1C, FADS2, INPP5B, ITGB3, NEURL4, NTRK1, PCAT1, TYK2, and VAV3. OS and DFS analyses were subsequently performed for these 10 genes. The results showed that ADM5, INPP5B, NEURL4, and TYK2 exhibited significant differences in DFS, with their upregulated expression associated with poorer disease-free survival (Fig. 4). These four genes were selected as target genes for further analysis, and protein expression levels were validated using the HPA (Fig. 5). ADM5 was identified as extracellularly expressed, thus lacking staining images. In contrast, INPP5B, NEURL4, and TYK2 showed lower expression in prostate cancer tissues compared to normal prostate tissues.

Table 5 Medication use (thyroid preparations) and Prostate cancer_MendelianRandomization

Exposure	Outcome	method	nsnp	b	se	pval
Medication use (thyroid preparations) ebi-a-GCST90018990	Prostate cancer ebi-a-GCST006085	IVW	115	− 0.0253	0.0123	0.0402
Medication use (thyroid preparations) ebi-a-GCST90018990	Prostate cancer ebi-a-GCST90018905	IVW	118	− 0.0434	0.0164	0.0081
Medication use (thyroid preparations) ebi-a-GCST90018990	Prostate cancer finn-b-C3_PROSTATE	IVW	116	− 0.0806	0.03023	0.0077
Medication use (thyroid preparations) ebi-a-GCST90018990	Prostate cancer ieu-b-85	IVW	113	− 0.0246	0.0123	0.0464

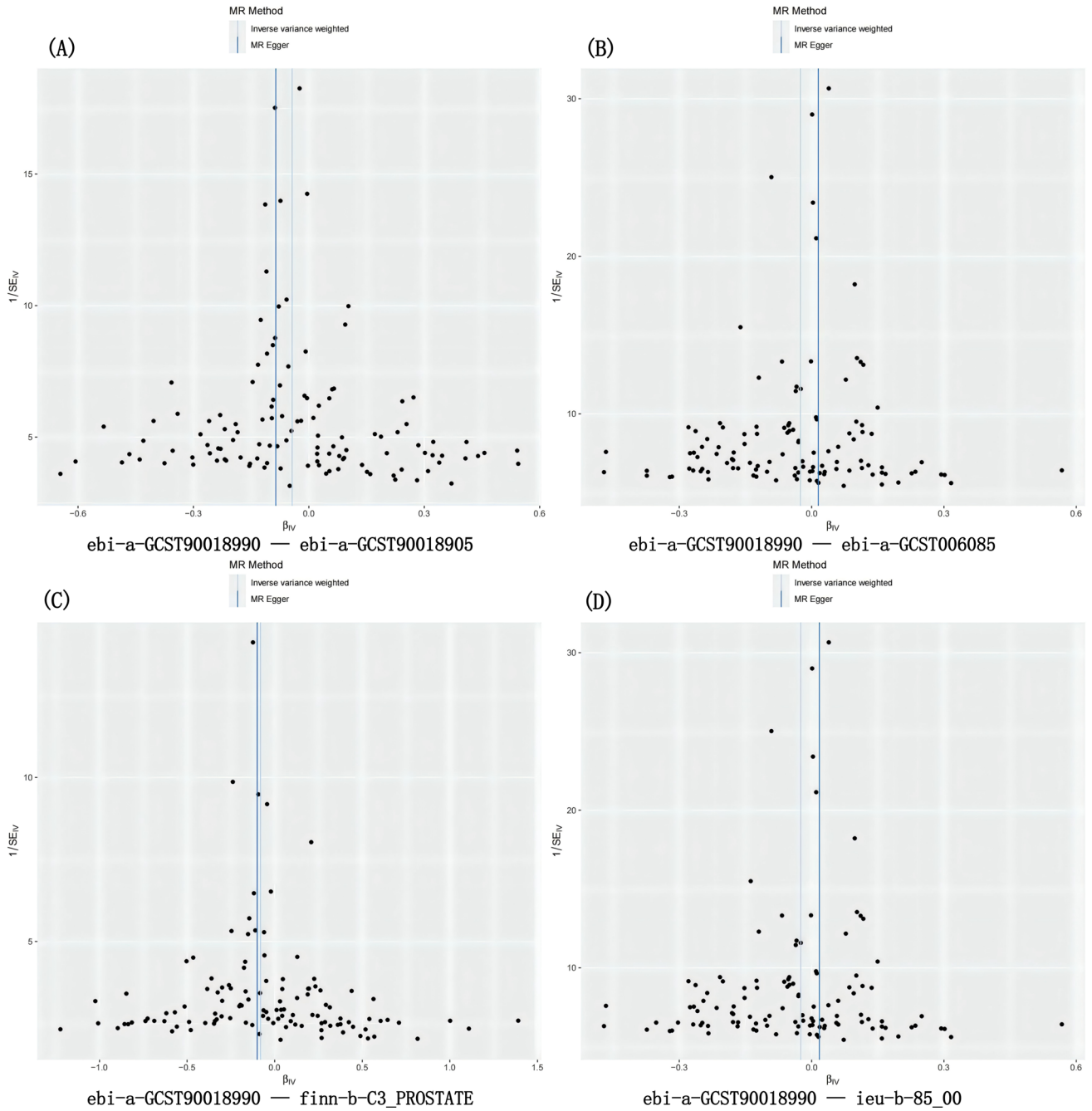

Fig. 3 Mendelian Randomization funnel plots for the association between Medication use (thyroid preparations) and prostate cancer

3.7 Relationship between INPP5B, NEURL4 and Tyk2 expression and immune cell infiltration in prostate cancer

Using TIMER2.0, the correlation between the expression levels of ADM5, INPP5B, NEURL4, and TYK2 and immune cell infiltration in prostate cancer was analyzed. Due to missing data for ADM5, only results for INPP5B, NEURL4, and TYK2 are presented (Figs. 6, 7, 8). Decreased INPP5B expression was positively correlated with the infiltration of B cells, CD4 + T cells, CD8 + T cells, myeloid dendritic cells, macrophages, neutrophils, monocytes, cancer-associated fibroblasts (CAFs), and natural killer (NK) cells in prostate cancer. Decreased NEURL4 expression was positively correlated with the infiltration of B cells, CD4 + T cells, CD8 + T cells, myeloid dendritic cells, macrophages, neutrophils, and NK cells. However, no

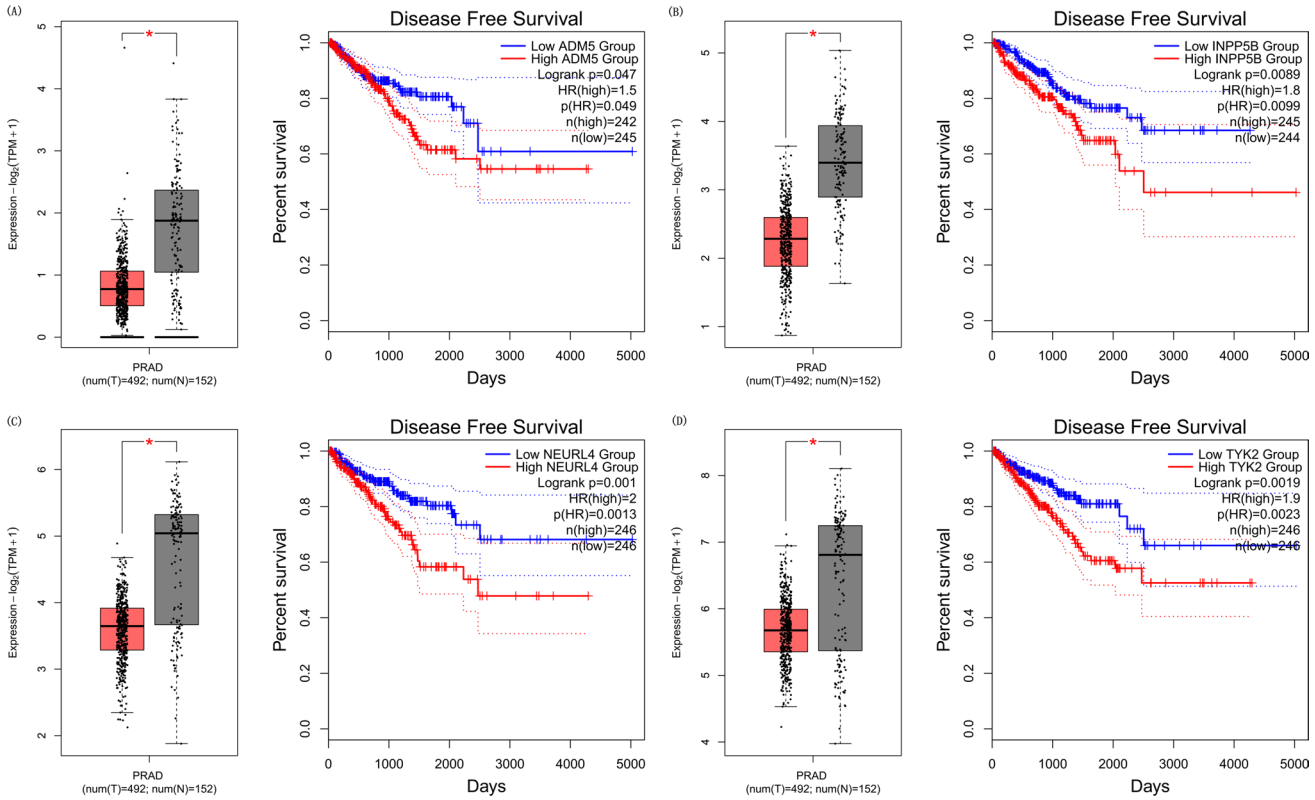

Fig. 4 Comparison of gene expression levels and their impact on DFS in prostate adenocarcinoma (PRAD). **A** ADM5: The boxplot on the left illustrates that ADM5 expression is significantly lower in tumor tissues (T, red, n = 492) compared to normal tissues (N, gray, n = 152) ($p < 0.05$, marked by a red asterisk). The Kaplan-Meier survival curve on the right shows that patients with high ADM5 expression (red) have significantly reduced disease-free survival (DFS) (Log-rank p = 0.047, HR = 1.5). **B** INPP5B: The boxplot on the left demonstrates significantly lower INPP5B expression in tumor tissues (red box). Kaplan-Meier analysis on the right indicates that patients with high INPP5B expression (red) have poorer DFS (Log-rank p = 0.0089, HR = 1.8). **C** NEURL4: The boxplot on the left shows significantly lower expression of NEURL4 in tumor tissues. Survival analysis on the right reveals that patients with high NEURL4 expression have significantly worse DFS (Log-rank p = 0.001, HR = 2). **D** TYK2: The boxplot on the left indicates a trend toward lower TYK2 expression in tumor tissues. Kaplan-Meier survival curves on the right demonstrate that patients with high TYK2 expression exhibit significantly reduced DFS (Log-rank p = 0.0019, HR = 1.9)

significant correlation was observed with monocytes or CAFs. Decreased TYK2 expression was positively correlated with the infiltration of B cells, CD4 + T cells, CD8 + T cells, myeloid dendritic cells, macrophages, neutrophils, monocytes, and NK cells. In contrast, it showed a negative correlation with CAF infiltration in prostate cancer.

3.8 Functional enrichment analysis

This study performed functional enrichment analysis of 10 differentially expressed genes using the Metascape platform to investigate their potential roles in biological processes, molecular functions, and associated pathways (Dataset_3). The results revealed significant enrichment in biological processes such as cell surface receptor protein tyrosine kinase signaling pathways (GO:0007169), response to injury (GO:0009611), and positive regulation of cell adhesion (GO:0045785), suggesting their involvement in the regulation of cell signaling, injury repair, and cell–cell interactions ($p < 0.01$, enrichment factor > 1.5).

Pathway and process enrichment analyses using KEGG, Reactome, and PANTHER databases demonstrated that several enriched pathways are closely related to cell signaling and immune regulation. High-density molecular functional modules were identified using the MCODE algorithm, and independent functional enrichment analysis of these modules revealed associations with signaling networks and cell cycle regulation, providing important insights into the cooperative roles of these genes.

Additionally, association analysis based on the DisGeNET database further identified strong links between these genes and multiple human diseases, particularly autoimmune diseases, hypothyroidism, and prostate cancer progression.

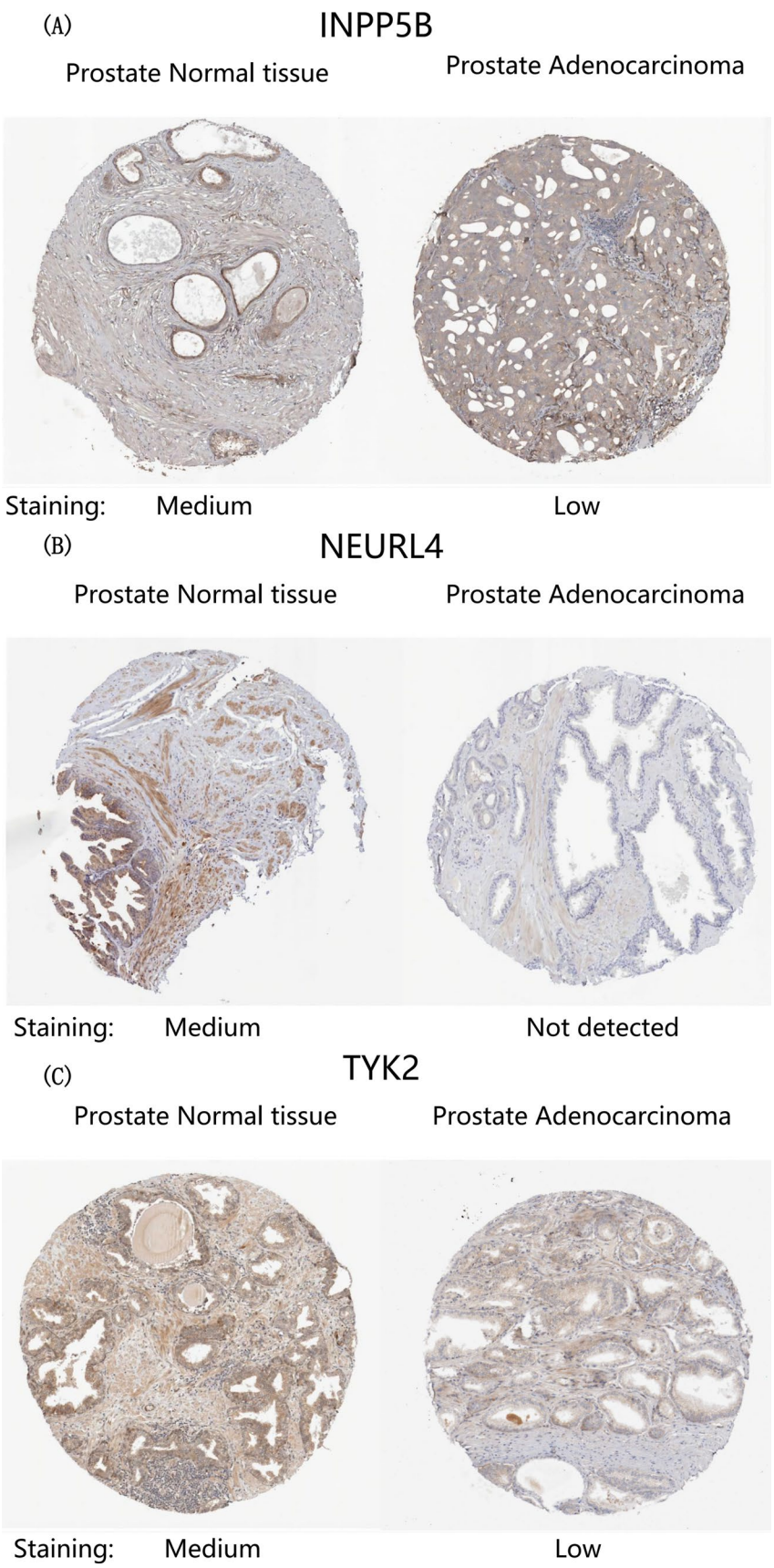

Fig. 5 Validation of INPP5B, NEURL4, and TYK2 protein expression in prostate adenocarcinoma and normal prostate tissues using the Human Protein Atlas database. **A** INPP5B: The left panel shows moderate (Medium) protein expression levels of INPP5B in normal prostate tissues. The right panel indicates reduced (Low) protein expression levels in prostate adenocarcinoma tissues. **B** NEURL4: The left panel shows moderate (Medium) protein expression levels of NEURL4 in normal prostate tissues. In contrast, NEURL4 protein expression is not detected (Not detected) in prostate adenocarcinoma tissues, as shown in the right panel. **C** TYK2: The left panel shows moderate (Medium) protein expression levels of TYK2 in normal prostate tissues. The right panel demonstrates reduced (Low) protein expression levels in prostate adenocarcinoma tissues

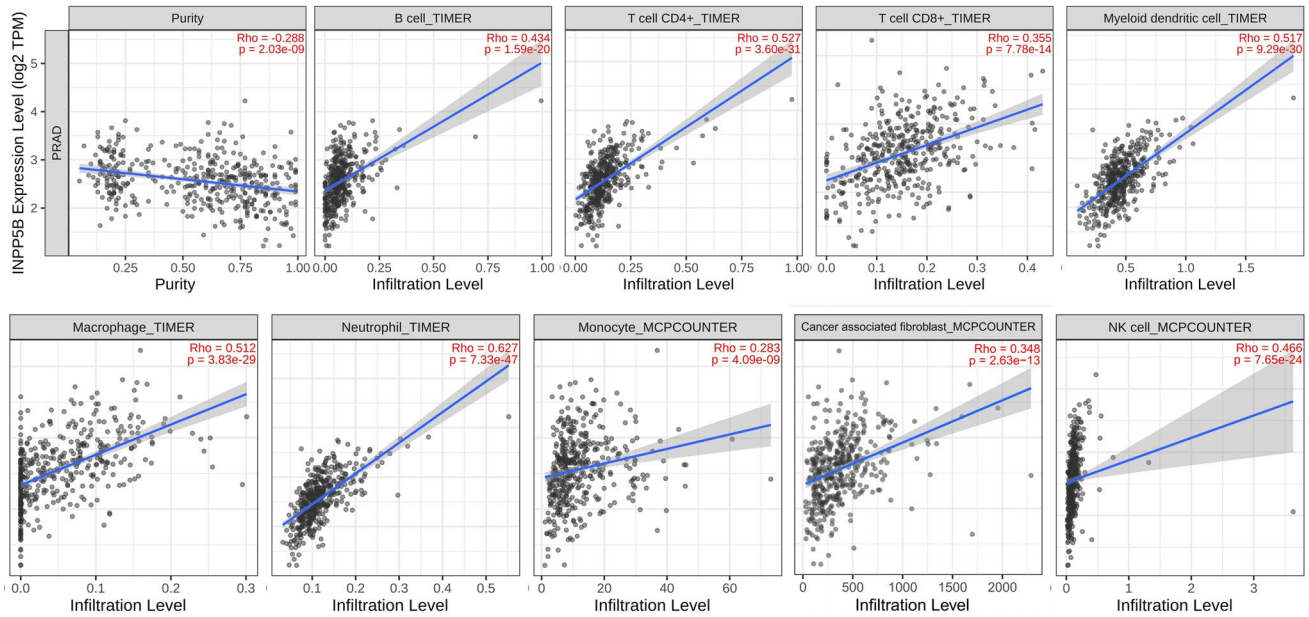

Fig. 6 Correlation between INPP5B expression and immune cell infiltration levels in Prostate cancer analyzed

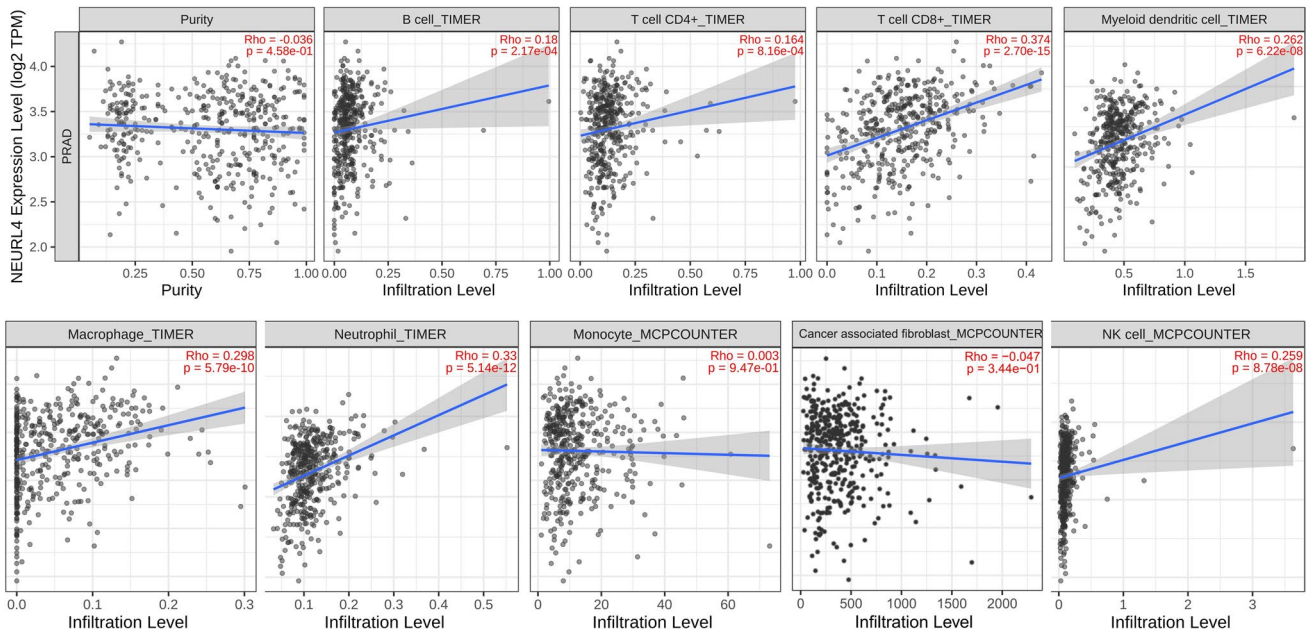

Fig. 7 Correlation between NEURL4 expression and immune cell infiltration levels in Prostate cancer analyzed

3.9 Clinical pathological staging analysis

Using the cBioPortal platform, the mRNA expression levels of ADM5, INPP5B, NEURL4, and TYK2 were systematically analyzed across prostate cancer samples at different clinical stages (AJCC stages T2A to T4) (Dataset_4).

For ADM5, significant differences in mRNA expression were observed among samples at different clinical stages. Notably, ADM5 expression displayed substantial heterogeneity at stage T3B. Shallow and deep deletions were often associated with lower expression levels, while copy number amplifications and gains did not significantly increase mRNA expression. At stage T4, due to the limited number of samples, a decreasing trend in expression was observed.

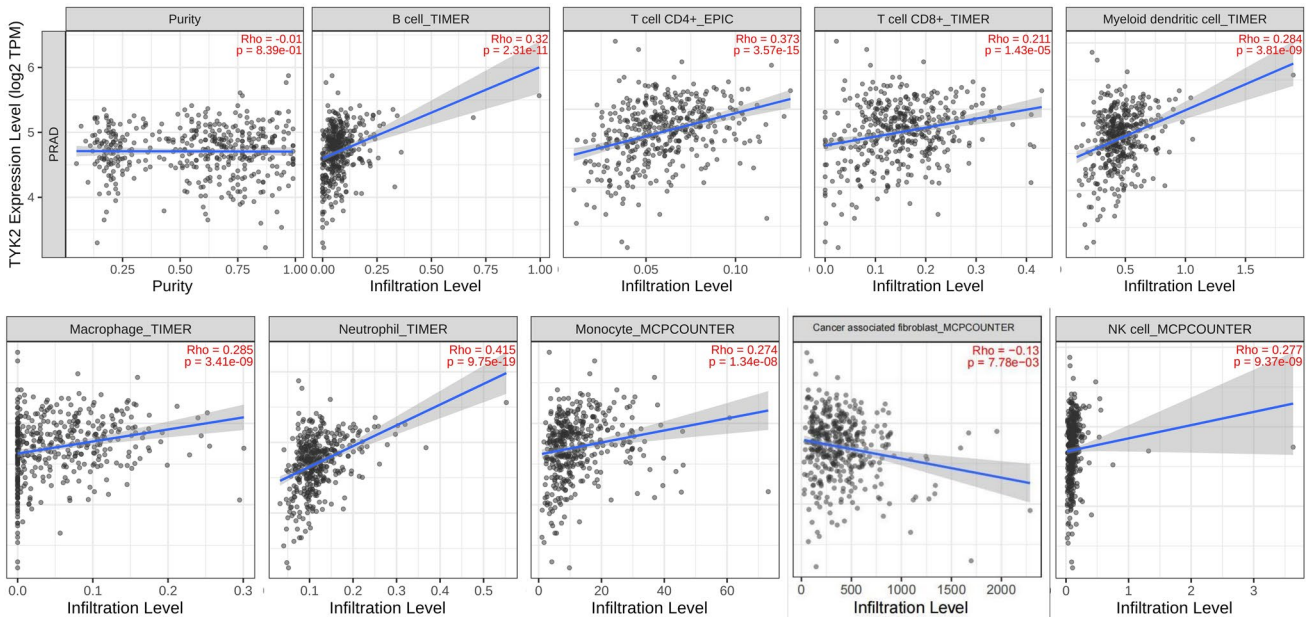

Fig. 8 Correlation between Tyk2 expression and immune cell infiltration levels in Prostate cancer analyzed

For INPP5B, mRNA expression levels varied across stages, with noticeable heterogeneity. Shallow deletions and copy number gains affected mRNA expression, particularly at stages T3B and T4, where expression changes were more pronounced.

NEURL4 showed significant differences in mRNA expression across clinical stages, with higher expression observed at stages T2C and T3A, and polarized expression levels at stage T4. Copy number deletions (both shallow and deep) significantly influenced mRNA expression, whereas missense mutations and copy number gains did not result in notable expression changes.

For TYK2, mRNA expression differences were evident across clinical stages, particularly at stages T3A and T3B, where copy number gains and amplifications appeared to upregulate mRNA expression. In contrast, shallow deletions were associated with relatively lower expression levels. At stage T4, the expression showed greater variability.

4 Discussion

This study systematically explored the association between thyroid hormones and prostate cancer using a comprehensive, multidimensional approach that included observational analysis of the NHANES database, MR analysis, and bioinformatics analysis. The results demonstrated a significant negative correlation between thyroid hormone levels (FT3 and T3) and prostate cancer risk. Furthermore, the use of thyroid preparation medications, which modulate thyroid hormone levels, was causally linked to a reduced risk of prostate cancer.

Bioinformatics analysis identified ADM5, INPP5B, NEURL4, and TYK2 as potential therapeutic targets for prostate cancer treatment. Building on these findings, this study provides an in-depth discussion of the biological plausibility, clinical relevance, and limitations of these results.

In the observational analysis, FT3 and T3 levels were significantly lower in the high-risk PCa group compared to the low-risk group. In the observational analysis, FT3 and T3 levels were significantly lower in the high-risk PCa group compared to the low-risk group. After adjusting for confounders, the association between thyroid hormone levels and prostate cancer risk remained, though it did not reach statistical significance. These results suggest a potential role of thyroid hormones in PCa progression, but the relationship appears to be more complex when adjusting for key factors such as age, PSA, and BMI. The borderline significance observed for T3 ($p = 0.052$) suggests that the association may become clearer with a larger sample size or more targeted data. This marginal result could be influenced by potential biases in public databases, such as variations in hormone measurements or unaccounted confounding factors. While the lack of statistical significance limits conclusions, it does not rule out the potential role of thyroid hormones in prostate cancer

risk, warranting further exploration. The sustained proliferation of cancer cells is heavily dependent on the Warburg effect, which primarily provides energy through aerobic glycolysis rather than mitochondrial respiration [31]. Thyroid hormones play a critical role in regulating cellular metabolism, apoptosis, and proliferation. Among these, T3 modulates cell differentiation and mitochondrial respiration by binding to nuclear thyroid hormone receptors and is regarded as a potential tumor suppressor [32]. In vitro studies have shown that T3 induces cellular senescence in prostate cancer cells via DEC1- and p15INK4B-dependent pathways [14]. Animal studies further demonstrate that T3 inhibits the release of invasion-promoting factors induced by adrenergic stimulation, thereby slowing the progression of prostate cancer [33]. FT3, the active form of T3, is the primary hormone mediating biological effects and more accurately reflects thyroid function [34]. By acting on nuclear receptors, FT3 regulates gene expression and metabolic activity. In this study, both T3 and FT3 were negatively associated with prostate cancer risk, supporting the protective role of thyroid hormones in prostate cancer development. The sustained proliferation of cancer cells is heavily dependent on the Warburg effect, which primarily provides energy through aerobic glycolysis rather than mitochondrial respiration [31]. Thyroid hormones play a critical role in regulating cellular metabolism, apoptosis, and proliferation. Among these, T3 modulates cell differentiation and mitochondrial respiration by binding to nuclear thyroid hormone receptors and is regarded as a potential tumor suppressor [32]. In vitro studies have shown that T3 induces cellular senescence in prostate cancer cells via DEC1- and p15INK4B-dependent pathways [14]. Animal studies further demonstrate that T3 inhibits the release of invasion-promoting factors induced by adrenergic stimulation, thereby slowing the progression of prostate cancer [33]. FT3, the active form of T3, is the primary hormone mediating biological effects and more accurately reflects thyroid function [34]. By acting on nuclear receptors, FT3 regulates gene expression and metabolic activity. In this study, both T3 and FT3 were negatively associated with prostate cancer risk, supporting the protective role of thyroid hormones in prostate cancer development.

Using GWAS data, MR analysis further validated the causal relationship between thyroid preparation use, which influences thyroid hormone levels, and reduced PCa risk. IVW analysis revealed a significant negative association between thyroid preparation use and PCa risk ($b < 0$, $p < 0.05$), suggesting that elevated thyroid hormone levels may serve as a key protective factor against PCa. These findings align with previous evidence that thyroid hormones, particularly T3, act as tumor suppressors by regulating mitochondrial activity and inducing cellular senescence [32]. Thus, thyroid preparations could have therapeutic potential in reducing prostate cancer risk.

Furthermore, bioinformatics analysis identified ADM5, INPP5B, NEURL4, and TYK2 as potential therapeutic targets for prostate cancer. ADM5 (Adrenomedullin 5), a newly identified peptide, regulates cardiovascular, immune, and fluid balance functions through receptor interactions [35]. In cancer, ADM promotes tumor progression in colorectal cancer by modulating angiogenesis and invasion [35] and exhibits anti-apoptotic effects by regulating Bcl-2 expression in osteosarcoma cells under hypoxic conditions [36]. These findings highlight ADM5's potential as a therapeutic target. INPP5B (Inositol Polyphosphate-5-Phosphatase B) is a multifunctional enzyme that influences intracellular signaling pathways, primarily through the dephosphorylation of inositol phosphates, particularly the tumor-associated PI3K/AKT pathway [37]. Recent studies have demonstrated that aberrant expression of INPP5B is closely associated with disease progression and prognosis in various cancers. For instance, INPP5B interacts with PTEN to regulate proliferation and migration in lung adenocarcinoma cells [38]. Additionally, in hepatocellular carcinoma, INPP5B cooperates with SYNJ2 to regulate cellular metabolism, potentially influencing tumor progression and chemotherapy response [39]. NEURL4 (Neuralized E3 Ubiquitin Protein Ligase 4) plays a critical role in cancer by regulating centrosome overduplication, which is associated with aggressive clinical features and poor prognosis [40]. NEURL4 interacts with HERC2 to modulate p53 activity and is frequently deleted in prostate cancer, underscoring its involvement in tumorigenesis [41]. Its expression correlates with chemotherapy response, suggesting a role in the tumor microenvironment and immune regulation [42]. TYK2 (Tyrosine Kinase 2), a Janus kinase family member, mediates critical cytokine and growth factor signaling pathways, regulating cell proliferation, differentiation, and survival [43, 44]. Studies on patients with a history of primary malignant tumors suggest that Tyk2 may be associated with the development of various cancers [45].TYK2 inhibition reduces invasiveness in prostate cancer cells [46], and its activation is associated with IL-6 and IL-10 signaling, highlighting its role in immune regulation [47, 48].

Functional enrichment analysis of the 10 differentially expressed genes revealed their significant involvement in key biological processes, including receptor tyrosine kinase signaling, response to damage, and positive regulation of cell adhesion. These processes are highly active in normal tissues, but their regulatory functions may be weakened in prostate cancer due to reduced gene expression. Low expression of receptor tyrosine kinase signaling genes may impair the ability of prostate cancer cells to respond to external signals, such as growth factors and environmental regulators, disrupting normal proliferation and differentiation while allowing abnormal signaling to promote uncontrolled tumor growth

[49]. Similarly, low expression of genes related to the response to damage indicates that prostate cancer cells may have diminished capacities to counter oxidative stress and repair DNA damage. This deficiency can lead to genomic instability and increased reliance on supportive mechanisms within the tumor microenvironment, such as inflammation, further driving tumor progression [50]. The reduced expression of genes involved in positive regulation of cell adhesion may disrupt cell–cell interactions and matrix-dependent signaling, allowing tumor cells to detach from the primary site and migrate to distant locations. This dysregulation is particularly relevant to the mechanisms underlying cancer cell invasion and metastasis, especially to the bone, which is a common site for prostate cancer metastasis [51]. Pathway enrichment analysis further highlighted the roles of these genes in cellular signaling pathways, such as the PI3K-Akt pathway, and immune regulatory pathways. In the PI3K-Akt pathway, low expression of these genes may fail to suppress proliferative signals or promote apoptosis, leading to rapid tumor growth and treatment resistance [52].

In immune regulatory pathways, reduced gene expression may impair immune cell function or decrease the sensitivity of tumor cells to immune attacks, enabling cancer cells to evade immune surveillance and dominate the immune microenvironment. High-density functional module analysis using the MCODE algorithm showed that these genes exhibit synergistic roles in signal transduction networks and cell cycle regulation. However, their low expression may disrupt the balance of critical molecular networks, providing an advantage to tumor-related abnormal signaling and accelerating malignant progression. The low expression of cell cycle regulatory modules may limit the normal function of key cell cycle regulators, enabling tumor cells to bypass cell cycle checkpoints and achieve uncontrolled proliferation. Association analysis using the DisGeNET database revealed that the low expression of these genes is closely linked to prostate cancer progression. Additionally, their association with chronic inflammation, autoimmune diseases, and hypothyroidism suggests that prostate cancer may involve broader mechanisms of inflammation or metabolic dysregulation.

High levels of immune cell infiltration are generally associated with favorable cancer prognosis. In prostate cancer, the infiltration of T cells (CD4 + and CD8 +) and other immune cells, such as B cells, macrophages, and neutrophils, indicates a robust antitumor immune response [53–55]. TIMER2.0 data were unavailable for ADM5; thus, the discussion focuses on INPP5B, NEURL4, and TYK2. Analysis revealed that low expression levels of these genes positively correlate with the infiltration of various immune cells in prostate cancer. INPP5B was positively correlated with the infiltration of B cells, CD4 + T cells, CD8 + T cells, dendritic cells, macrophages, neutrophils, monocytes, and NK cells, suggesting that its low expression may promote immune cell infiltration and help regulate the tumor immune microenvironment. NEURL4 was positively associated with most immune cells but showed no significant correlation with monocytes or cancer-associated fibroblasts, indicating a cell-specific role in immune microenvironment regulation. TYK2 was positively correlated with the infiltration of B cells, CD4 + T cells, and NK cells but negatively correlated with cancer-associated fibroblast infiltration, suggesting a potential role in suppressing stromal responses within the tumor microenvironment.

Systematic mRNA expression analysis of ADM5, INPP5B, NEURL4, and TYK2 across prostate cancer stages (AJCC stages T2A–T4) using cBioPortal revealed significant stage-specific differences. ADM5 showed considerable heterogeneity in T3B and a downward trend in T4, indicating regulation by multiple factors during cancer progression. Shallow and deep copy number deletions were associated with reduced expression, while copy number gains and amplifications did not significantly increase ADM5 mRNA levels, suggesting that copy number alterations are not the primary driver of its expression. INPP5B displayed notable expression changes in T3B and T4 stages, indicating its role in the transition from localized to invasive cancer. Its stage-specific expression suggests a molecular switch-like function, influenced by distinct regulatory contexts. NEURL4 showed increased expression at T2C and T3A stages, reflecting its involvement in maintaining balance in cellular regulation and signaling pathways during early tumor development. At T4, NEURL4 exhibited polarized expression patterns, with some samples showing significant upregulation and others significant downregulation, possibly due to data limitations or the formation of tumor subtypes in advanced stages. Copy number deletions significantly affected NEURL4 expression, while missense mutations and copy number gains had no notable impact, indicating a primary role for copy number changes in its regulation. TYK2 expression was upregulated in T3A and T3B stages due to copy number gains and amplifications, suggesting a key role in promoting tumor invasiveness. Conversely, TYK2 expression was significantly reduced in samples with shallow deletions, further supporting the hypothesis of copy number-dependent regulation. The high variability of TYK2 expression in T4 samples may reflect the molecular heterogeneity or complex regulatory mechanisms of advanced-stage tumors.

Despite the robust findings, this study has several limitations. First, the NHANES database is cross-sectional, which precludes establishing temporal causality between thyroid hormone levels and prostate cancer risk. Second, the genetic instruments used in MR analysis may not fully capture the biological complexity of thyroid hormones, and the findings are limited to European populations, introducing potential racial bias. Third, bioinformatics analyses were based on publicly available datasets, and the reproducibility of these results in experimental models and mechanistic validation remain to

be explored. Fourth, the potential interactions between thyroid hormones and other prostate cancer risk factors, such as diet, obesity, and genetic predisposition, were not fully addressed in this study. Future research should address these interactions in greater depth.

This study systematically revealed a negative correlation between thyroid hormone levels (FT3 and T3) and prostate cancer risk and further explored causal relationships and potential therapeutic targets through MR analysis and bioinformatics methods. These findings offer new perspectives on the mechanisms underlying prostate cancer, providing a foundation for risk prediction, biomarker development, and personalized therapeutic strategies. Future studies should incorporate large-scale prospective cohorts and experimental validation to investigate the mechanistic role of thyroid hormones in prostate cancer and their clinical applications. Moreover, functional studies of differentially expressed genes such as ADM5, INPP5B, NEURL4, and TYK2 may offer novel directions for developing targeted therapies.

5 Conclusion

We propose that there is a potential negative correlation between thyroid hormones T3 and FT3 and prostate cancer risk, with evidence suggesting a causal relationship. Through MR analysis, ADM5, INPP5B, NEURL4, and TYK2 were identified as key genes potentially associated with prostate cancer, providing significant insights into disease risk prediction, biomarker development, and personalized therapeutic strategies. Future functional studies of these genes may offer novel directions for the development of targeted therapies for prostate cancer.

Acknowledgements Our research has greatly benefited from the resources provided by the NHANES database, the foundational genetic data from genome-wide association studies (GWAS), and the extensive genomic datasets available through The Cancer Genome Atlas (TCGA). We are also grateful for the expression analysis capabilities of the GEPIA2 platform, as well as the functional enrichment analyses provided by Metascape and the immune infiltration analysis tools of TIMER2.0. Additionally, we extend our appreciation to The Human Protein Atlas and cBioPortal for their invaluable support in protein function analysis and data management, which significantly contributed to our study.

Author contributions The contributions of the authors to this work are as follows: Jin-hai Wu was responsible for the conception and design of the study. Administrative support was provided by Bin Wang and Xue-jin Zhu. Study materials or patient recruitment were provided by Xi-heng Zheng, Yan-fei Chen and Ran Xu. The collection and assembly of data were carried out by Jin-hai Wu and Jia-din Guo. Data analysis and interpretation were performed by Jin-hai Wu, Si-an Chen, Xue-jin Zhu, and Jing Li. The manuscript was written collaboratively by Jin-hai Wu, and the final approval of the manuscript was provided by all authors.

Funding This work was supported by the Guangzhou Medical and Health Science and Technology Project (20231A011103). General projects of Guangzhou municipal Science and Technology Bureau (2023A04J0598), Guangdong Basic and Applied Basic Research Foundation (2022A1515111122).

Data availability The data analyzed in this study were obtained from the following publicly available repositories: National Health and Nutrition Examination Survey (NHANES): https://wwwn.cdc.gov/nchs/nhanes/Default.aspx. Genome-Wide Association Studies (GWAS) Catalog: https://www.ebi.ac.uk/gwas/. Human Protein Atlas (HPA): https://www.proteinatlas.org/. GEPIA2 (Gene Expression Profiling Interactive Analysis 2): http://gepia2.cancer-pku.cn/#index. Metascape: https://metascape.org/gp/index.html#/main/step1. TIMER2.0 Database: http://timer.comp-genomics.org/. cBioPortal for Cancer Genomics: https://www.cbioportal.org/. The data that support the findings of this study are available in these repositories and were derived from the aforementioned public domain resources.

Declarations

Ethics approval and consent to participate All data used in this study were obtained from public databases; therefore, ethical approval was not required.

Consent for publication All the authors agree on the publication of the results of the present manuscript.

Competing interests The authors declare no competing interests.

References

1. Culp MB, Soerjomataram I, Efstathiou JA, Bray F, Jemal A. Recent global patterns in prostate cancer incidence and mortality rates. Eur Urol. 2020;77(1):38–52. https://doi.org/10.1016/j.eururo.2019.08.005.
2. Negoita S, Mariotto A, Benard V, Kohler BA, Jemal A, Penberthy L. Reply to annual report to the nation on the status of cancer, part II: recent changes in prostate cancer trends and disease characteristics. Cancer. 2019;125(2):318–9. https://doi.org/10.1002/cncr.31845.
3. Demichelis F, Stanford JL. Genetic predisposition to prostate cancer: update and future perspectives. Urol Oncol. 2015;33(2):75–84. https://doi.org/10.1016/j.urolonc.2014.04.021.
4. Yeyeodu ST, Kidd LR, Kimbro KS. Protective innate immune variants in racial/ethnic disparities of breast and prostate cancer. Cancer Immunol Res. 2019;7(9):1384–9. https://doi.org/10.1158/2326-6066.CIR-18-0564.
5. de Bono JS, Guo C, Gurel B, De Marzo AM, Sfanos KS, Mani RS, et al. Prostate carcinogenesis: inflammatory storms. Nat Rev Cancer. 2020;20(8):455–69. https://doi.org/10.1038/s41568-020-0267-9.
6. Matsushita M, Fujita K, Nonomura N. Influence of diet and nutrition on prostate cancer. Int J Mol Sci. 2020;21(4):1447. https://doi.org/10.3390/ijms21041447.
7. Sung H, Ferlay J, Siegel RL, Laversanne M, Soerjomataram I, Jemal A, et al. Global cancer statistics 2020: GLOBOCAN estimates of incidence and mortality worldwide for 36 cancers in 185 countries. CA Cancer J Clin. 2021;71(3):209–49. https://doi.org/10.3322/caac.21660.
8. Gandaglia G, Leni R, Bray F, Fleshner N, Freedland SJ, Kibel A, et al. Epidemiology and prevention of prostate cancer. Eur Urol Oncol. 2021;4(6):877–92. https://doi.org/10.1016/j.euo.2021.09.006.
9. Orsted DD, Nordestgaard BG, Jensen GB, Schnohr P, Bojesen SE. Prostate-specific antigen and long-term prediction of prostate cancer incidence and mortality in the general population. Eur Urol. 2012;61(5):865–74. https://doi.org/10.1016/j.eururo.2011.11.007.
10. Catalona WJ, Partin AW, Slawin KM, Brawer MK, Flanigan RC, Patel A, et al. Use of the percentage of free prostate-specific antigen to enhance differentiation of prostate cancer from benign prostatic disease: a prospective multicenter clinical trial. JAMA. 1998;279(19):1542–7. https://doi.org/10.1001/jama.279.19.1542.
11. Krashin E, Piekiełko-Witkowska A, Ellis M, Ashur-Fabian O. Thyroid hormones and cancer: a comprehensive review of preclinical and clinical studies. Front Endocrinol (Lausanne). 2019;10:59. https://doi.org/10.3389/fendo.2019.00059.
12. Hercbergs AH, Ashur-Fabian O, Garfield D. Thyroid hormones and cancer: clinical studies of hypothyroidism in oncology. Curr Opin Endocrinol Diabetes Obes. 2010;17(5):432–6. https://doi.org/10.1097/MED.0b013e32833d9710.
13. Chan YX, Knuiman MW, Divitini ML, Brown SJ, Walsh J, Yeap BB. Lower TSH and higher free thyroxine predict incidence of prostate but not breast, colorectal or lung cancer. Eur J Endocrinol. 2017;177(4):297–308. https://doi.org/10.1530/EJE-17-0197.
14. Kotolloshi R, Mirzakhani K, Ahlburg J, Kraft F, Pungsrinont T, Baniahmad A. Thyroid hormone induces cellular senescence in prostate cancer cells through induction of DEC1. J Steroid Biochem Mol Biol. 2020;201: 105689. https://doi.org/10.1016/j.jsbmb.2020.105689.
15. Davies NM, Holmes MV, Davey SG. Reading Mendelian randomisation studies: a guide, glossary, and checklist for clinicians. BMJ. 2018;362: k601. https://doi.org/10.1136/bmj.k601.
16. Skrivankova VW, Richmond RC, Woolf BAR, Davies NM, Swanson SA, VanderWeele TJ, et al. Strengthening the reporting of observational studies in epidemiology using Mendelian randomisation (STROBE-MR): explanation and elaboration. BMJ. 2021;375: n2233. https://doi.org/10.1136/bmj.n2233.
17. Hemani G, Zheng J, Elsworth B, Wade KH, Haberland V, Baird D, et al. The MR-Base platform supports systematic causal inference across the human phenome. Elife. 2018;7:e34408. https://doi.org/10.7554/eLife.34408.
18. Liu Y, He JX, Ji B, et al. Comprehensive analysis of integrin αvβ3/α6β1 in prognosis and immune escape of prostate cancer. Aging (Albany NY). 2023;15(20):11369–88. https://doi.org/10.18632/aging.205131.
19. Miao S, Bao C, Zhang Y, Wang L, Jin X, Huang B, et al. Associations of the Geriatric Nutritional Risk Index with high risk for prostate cancer: a cross-sectional study. Nutrition. 2023;115: 112164. https://doi.org/10.1016/j.nut.2023.112164.
20. Zhou CK, Check DP, Lortet-Tieulent J, Laversanne M, Jemal A, Ferlay J, et al. Prostate cancer incidence in 43 populations worldwide: an analysis of time trends overall and by age group. Int J Cancer. 2016;138(6):1388–400. https://doi.org/10.1002/ijc.29894.
21. DecisionLinnc Core Team. DecisionLinnc. 1.0. November 2023. DecisionLinnc is a platform that integrates multiple programming language environments and enables data processing, data analysis, and machine learning through a visual interface. Hangzhou, CHN. Available from: https://www.statsape.com/.
22. Burgess S, Small DS, Thompson SG. A review of instrumental variable estimators for Mendelian randomization. Stat Methods Med Res. 2017;26(5):2333–55. https://doi.org/10.1177/0962280215597579.
23. Burgess S, Bowden J, Fall T, Ingelsson E, Thompson SG. Sensitivity analyses for robust causal inference from Mendelian randomization analyses with multiple genetic variants. Epidemiology. 2017;28(1):30–42. https://doi.org/10.1097/EDE.0000000000000559.
24. Cunningham F, Allen JE, Allen J, Alvarez-Jarreta J, Amode MR, Armean IM, et al. Ensembl 2022. Nucleic Acids Res. 2022;50(D1):D988–95. https://doi.org/10.1093/nar/gkab1049.
25. Siegel RL, Miller KD, Jemal A. Cancer statistics, 2019. CA Cancer J Clin. 2019;69(1):7–34. https://doi.org/10.3322/caac.21551.
26. Zhou Y, Zhou B, Pache L, Chang M, Khodabakhshi AH, Tanaseichuk O, et al. Metascape provides a biologist-oriented resource for the analysis of systems-level datasets. Nat Commun. 2019;10(1):1523. https://doi.org/10.1038/s41467-019-09234-6.
27. Uhlén M, Fagerberg L, Hallström BM, Lindskog C, Oksvold P, Mardinoglu A, et al. Proteomics. Tissue-based map of the human proteome. Science. 2015;347(6220):1260419. https://doi.org/10.1126/science.1260419.
28. Li T, Fu J, Zeng Z, Cohen D, Li J, Chen Q, et al. TIMER2.0 for analysis of tumor-infiltrating immune cells. Nucleic Acids Res. 2020;48(W1):W509–14. https://doi.org/10.1093/nar/gkaa407.
29. Gao J, Aksoy BA, Dogrusoz U, Dresdner G, Gross B, Sumer SO, et al. Integrative analysis of complex cancer genomics and clinical profiles using the cBioPortal. Sci Signal. 2013;6(269):pl1. https://doi.org/10.1126/scisignal.2004088.
30. Hoadley KA, Yau C, Hinoue T, Wolf DM, Lazar AJ, Drill E, et al. Cell-of-origin patterns dominate the molecular classification of 10,000 tumors from 33 types of cancer. Cell. 2018;173(2):291-304.e6. https://doi.org/10.1016/j.cell.2018.03.022.

31. Vander Heiden MG, Cantley LC, Thompson CB. Understanding the Warburg effect: the metabolic requirements of cell proliferation. Science. 2009;324(5930):1029–33. https://doi.org/10.1126/science.1160809.
32. Goemann IM, Romitti M, Meyer ELS, Wajner SM, Maia AL. Role of thyroid hormones in the neoplastic process: an overview. Endocr Relat Cancer. 2017;24(11):R367–85. https://doi.org/10.1530/ERC-17-0192.
33. Delgado-González E, Aceves C, Anguiano B. Triiodothyronine (T3) supplementation prevents the overexpression of invasion factors induced by β-adrenergic stimulation in prostate cancer models. Cancer Res. 2012;72(4 Suppl):C62. https://doi.org/10.1158/1538-7445.PRCA2012-C62.
34. Wenzel KW. Pharmacological interference with in vitro tests of thyroid function. Metabolism. 1981;30(7):717–32. https://doi.org/10.1016/0026-0495(81)90089-5.
35. Wang L, Gala M, Yamamoto M, Pino MS, Kikuchi H, Shue DS, et al. Adrenomedullin is a therapeutic target in colorectal cancer. Int J Cancer. 2014;134(9):2041–50. https://doi.org/10.1002/ijc.28542.
36. Wu XY, Hao CP, Ling M, Guo CH, Ma W. Hypoxia-induced apoptosis is blocked by adrenomedullin via upregulation of Bcl-2 in human osteosarcoma cells. Oncol Rep. 2015;34(2):787–94. https://doi.org/10.3892/or.2015.4011.
37. Pérez-Alea M, Vivancos A, Caratú G, Matito J, Ferrer B, Hernandez-Losa J, et al. Genetic profile of GNAQ-mutated blue melanocytic neoplasms reveals mutations in genes linked to genomic instability and the PI3K pathway. Oncotarget. 2016;7(19):28086–95. https://doi.org/10.18632/oncotarget.8578.
38. Deng J, Lin X, Li Q, Cai XY, Wu LW, Wang W, et al. Decreased INPP5B expression predicts poor prognosis in lung adenocarcinoma. Cancer Cell Int. 2022;22(1):189. https://doi.org/10.1186/s12935-022-02609-8.
39. Zhang R, Mo WJ, Huang LS, Chen JT, Wu WZ, He WY, et al. Identifying the prognostic risk factors of synaptojanin 2 and its underlying perturbations pathways in hepatocellular carcinoma. Bioengineered. 2021;12(1):855–74. https://doi.org/10.1080/21655979.2021.1890399.
40. Denu RA, Burkard ME. Analysis of the "centrosome-ome" identifies MCPH1 deletion as a cause of centrosome amplification in human cancer. Sci Rep. 2020;10(1):11921. https://doi.org/10.1038/s41598-020-68629-4.
41. Schneider T, Martinez-Martinez A, Cubillos-Rojas M, Bartrons R, Ventura F, Rosa JL. Large HERCs function as tumor suppressors. Front Oncol. 2019;9:524. https://doi.org/10.3389/fonc.2019.00524.
42. Katayama MLH, Vieira RADC, Andrade VP, Roela RA, Lima LGCA, Kerr LM, et al. Stromal cell signature associated with response to neoadjuvant chemotherapy in locally advanced breast cancer. Cells. 2019;8(12):1566. https://doi.org/10.3390/cells8121566.
43. Verma A, Kambhampati S, Parmar S, Platanias LC. Jak family of kinases in cancer. Cancer Metastasis Rev. 2003;22(4):423–34. https://doi.org/10.1023/a:1023805715476.
44. Hebenstreit D, Horejs-Hoeck J, Duschl A. JAK/STAT-dependent gene regulation by cytokines. Drug News Perspect. 2005;18(4):243–9. https://doi.org/10.1358/dnp.2005.18.4.908658.
45. Pritchard AL, Johansson PA, Nathan V, Howlie M, Symmons J, Palmer JM, et al. Germline mutations in candidate predisposition genes in individuals with cutaneous melanoma and at least two independent additional primary cancers. PLoS ONE. 2018;13(4): e0194098. https://doi.org/10.1371/journal.pone.0194098.
46. Ide H, Nakagawa T, Terado Y, Kamiyama Y, Muto S, Horie S. Tyk2 expression and its signaling enhances the invasiveness of prostate cancer cells. Biochem Biophys Res Commun. 2008;369(2):292–6. https://doi.org/10.1016/j.bbrc.2007.08.160.
47. Ge D, Gao AC, Zhang Q, Liu S, Xue Y, You Z. LNCaP prostate cancer cells with autocrine interleukin-6 expression are resistant to IL-6-induced neuroendocrine differentiation due to increased expression of suppressors of cytokine signaling. Prostate. 2012;72(12):1306–16. https://doi.org/10.1002/pros.22479.
48. Stearns ME, Hu Y, Wang M. IL-10 signaling via IL-10E1 is dependent on tyrosine phosphorylation in the IL-10R alpha chain in human primary prostate cancer cell lines. Oncogene. 2003;22(24):3781–91. https://doi.org/10.1038/sj.onc.1206579.
49. Lien EC, Dibble CC, Toker A. PI3K signaling in cancer: beyond AKT. Curr Opin Cell Biol. 2017;45:62–71. https://doi.org/10.1016/j.ceb.2017.02.007.
50. Chen H, Zhou L, Wu X, Li R, Wen J, Sha J, et al. The PI3K/AKT pathway in the pathogenesis of prostate cancer. Front Biosci (Landmark Ed). 2016;21(5):1084–91. https://doi.org/10.2741/4443.
51. Shukla S, Maclennan GT, Hartman DJ, Fu P, Resnick MI, Gupta S. Activation of PI3K-Akt signaling pathway promotes prostate cancer cell invasion. Int J Cancer. 2007;121(7):1424–32. https://doi.org/10.1002/ijc.22862.
52. Chang L, Graham PH, Hao J, Ni J, Bucci J, Cozzi PJ, et al. PI3K/Akt/mTOR pathway inhibitors enhance radiosensitivity in radioresistant prostate cancer cells through inducing apoptosis, reducing autophagy, suppressing NHEJ and HR repair pathways. Cell Death Dis. 2014;5(10): e1437. https://doi.org/10.1038/cddis.2014.415.
53. Andersen LB, Nørgaard M, Rasmussen M, Fredsøe J, Borre M, Ulhøi BP, et al. Immune cell analyses of the tumor microenvironment in prostate cancer highlight infiltrating regulatory T cells and macrophages as adverse prognostic factors. J Pathol. 2021;255(2):155–65. https://doi.org/10.1002/path.5757.
54. Davidsson S, Ohlson AL, Andersson SO, Fall K, Meisner A, Fiorentino M, et al. CD4 helper T cells, CD8 cytotoxic T cells, and FOXP3(+) regulatory T cells with respect to lethal prostate cancer. Mod Pathol. 2013;26(3):448–55. https://doi.org/10.1038/modpathol.2012.164.
55. Wu Z, Chen H, Luo W, Zhang H, Li G, Zeng F, et al. The landscape of immune cells infiltrating in prostate cancer. Front Oncol. 2020;10:517637. https://doi.org/10.3389/fonc.2020.517637.